Journal of Analytical and Applied Pyrolysis 161 (2022) 105385

Contents lists available at ScienceDirect

Journal of Analytical and Applied Pyrolysis

journal homepage: www.elsevier.com/locate/jaap

Autocatalytic influence of different levels of arsine on the thermal stability and pyrolysis of polypropylene

Hernández-Fernández Joaquin [a,b,*], Lopez-Martinez Juan [c]

[a] Centro de investigación en Ciencias e Ingenierías, CECOPAT&A, Cartagena, Colombia
[b] Department of Natural and Exact Sciences, Universidad de la Costa, Barranquilla, Colombia
[c] Universitat Politecnica de Valencia (UPV), Institute of Materials Technology (ITM), Plaza Ferrándiz and Carbonell s/n, 03801 Alcoy, Alicante, Spain

ARTICLE INFO

Keywords:
Arsine
Virgin polypropylene
Autocatalysis
Degradation start
Free radicals
Pyrolysis

ABSTRACT

In this article, the pyrolysis and thermo-degradation of 11 virgin-polypropylene (virgin-PP) with different levels of arsenic in its polymer matrix, was carried out in a discontinuous quartz reactor at 500 °C. To quantify arsine (AsH_3), 4 points were sampled during the PP synthesis process and a methodology was applied by GC with 4 detectors, which simultaneously and with a single injection allowed to quantify multiple components. AsH_3 in propylene varied between 0.05 and 4.73 ppm and arsenic in virgin-PP residues between 0.001 and 4.32 ppm for PP0 and PP10. These generated an increase in the melt flow index from 3.0 to 24.51 and maintained a direct relationship with an R^2 of 0.9993. The origin of thermo-oxidative degradation and the beginnings of virgin-PP pyrolysis are explained by the formation to aldehyde, ketone, alcohol, carboxylic acid functional groups, CO and CO_2. These species caused TG and DTG curves to have atypical behavior for PP. For example, PP10 with an arsenic content of 4.32 ppm presented 3 degradation peaks at 80, 90 and 200 °C with a mass loss ratio of 22%, 18% and 55% $°C^{-1}$ respectively. During pyrolysis the highest percentage of alkanes was found in PP0 with an average value of 62.4%, and the lowest values were found in PP8 to PP10, with oscillations between 0% and 1.4%. The total concentration of oxidized species for PP0 to PP10 was 2.26%, 32.7%, 43.1%, 50.9%, 59.3%, 66.2%, 75.0%, 83.0%, 89.1% and 97.5% respectively. In an O_2 atmosphere ketones and carboxylic acids were only identified in PP0 to PP5. CO_2 concentrations in PP5 to PP10 were of 100%.

1. Introduction

Industrial polypropylene (PP) residues are associated with pre-consumer PP or virgin-PP resins that are discarded or reprocessed during industrial production due to not complying with the physicochemical parameters that prevent their final purpose. The formation of these PP residues is related to failures in process controls or by the presence of chemical impurities in the raw materials required for their synthesis. Raw materials such as propylene, nitrogen and hydrogen have presented traces of impurities such as sulfides, mercaptans, hydrocarbons, oxygenates and arsine [1]. Arsine (AsH_3) is a compound of an inorganic chemical nature [2] and its formation in liquefied petroleum gas is associated with natural processes in geothermal vapor [2]. Organometallic complexes of phosphine and AsH_3 are widely applied in catalytic processes [3–8]. Inhibitors of polymerization reactions such as AsH_3, irreversibly affect the catalytic system and its coordination reaction with the active center of Ti in the catalyst, the different surfaces of $MgCl_2$ and with the Al-alkyl cocatalyst [9–11]. AsH_3 and other impurities have been studied during synthesis of PP and its impact has been quantified as inhibitors of Zieglar-Natta (ZN) catalysts [12–18], but not its impact on the onset of PP degradation, and understanding the chemistry of AsH_3 and the possible reactions that it may have during the polymerization of PP will allow to propose the most appropriate reaction mechanisms that let us to explain how arsine can affect the thermal stability of PP. The titanium (IV) chloride ($TiCl_4$) of the ZN catalyst tends to form multiple complexes with a wide variety of ligands, as a result of being a strong Lewis acid [19,20]. Most are of six coordinates $[TiCl_4L_2]$ or [$TiCl_4$ (L – L)] (L 1/4 single-toothed, L–L 1/4 bi-toothed ligand), but with very few $(AsH_3)_2$ ligands [19]. Degradation and pyrolysis of PP has been highly studied by degradation mechanisms promoted by external environmental effects such as UV rays, temperature, gamma rays, use of catalysts fluidized catalytic cracking (FCC), Zeolite Socony Mobil – 5 (ZSM5), CaC_2, alumina, $Mg(OH)_2$, ZnO, etc [21–35], where degradation occurs by homolytic rupture of the PP chain, of oxygen or hydrogen, to

* Corresponding author at: Department of Natural and Exact Sciences, Universidad de la Costa, Barranquilla, Colombia.
E-mail address: joaquin.hernandez@cecopat.com (H.-F. Joaquin).

https://doi.org/10.1016/j.jaap.2021.105385
Received 9 August 2021; Received in revised form 13 November 2021; Accepted 15 November 2021
Available online 27 November 2021

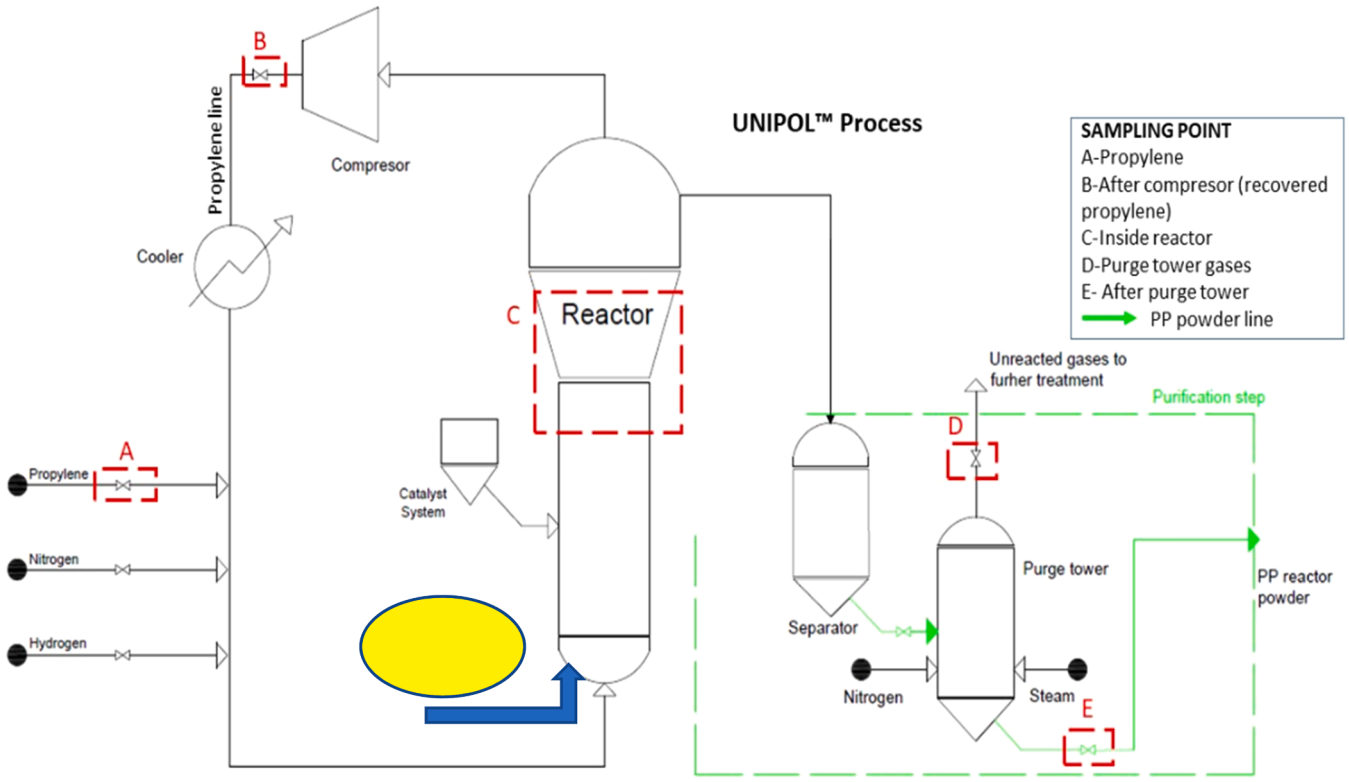

Fig. 1. Sampling points during the PP production process.

form free radicals and start degradation [36–51]. An alternative route for the onset of virgin-PP degradation has been based on the hydrolysis of ZN catalyst residuals and triethylaluminium (TEAl) co-catalyst, to give rise to the ethyl radical and become the initiator of virgin-PP waste degradation and pyrolysis [52]. This ethyl radical promotes the formation of aldehydes, ketones, carboxylic acids, alcohols, alkanes, alkenes, and increases CO_2 production between 49% and 66% [52]. No scientific literature was identified on the quantification of AsH_3 and arsenic in PP residues and their impact on the onset of virgin-PP degradation, making it necessary to explore its analysis techniques and propose a new analytical methodology. Current analysis methodologies for AsH_3 and arsenic refer to desorption/dissolution using dilute nitric acid, followed by analysis using graphite furnace–atomic absorption spectroscopy (GF–AAS), GC-MS (Gas chromatography with mass detector), a flame photometric detector, ion chromatography-inductively coupled plasma mass spectrometry, a dielectric barrier discharge detector and the use of GC with other means of detection [53–58].

This research studies the impact of different concentrations of AsH_3 on the onset of degradation and pyrolysis of virgin-PP. The effect of different levels of AsH_3 on the MFI will be determined. The arsenic content in the PP matrix will be quantified by X-ray fluorescence and its impact on the degradation of PP will be determined with TG and DTG. The effect of AsH_3 on the thermo-oxidation and pyrolysis of PP will also be determined by characterizing the gases formed in each heat treatment and the concentration of the gases will be quantified by gas chromatography with MS (mass), flame ionization detector (FID) and pulsed discharge helium ionization detector (PDHID) detectors. The research was conducted over a period of 5 consecutive years where sampling was carried out at different stages of the newly synthesized virgin-PP synthesis process, to identify the presence of AsH_3.

2. Materials and methods

2.1. Standard

The standards of interest were those of arsine, oxygenated derivatives and permanent gases.

5.15 ppm of AsH_3 in propylene balance. 5,0 ppm CO_2, 5049 CO, 4,96 ppm H_2, and 5,13 ppm O_2, in He balance. 45.32 ppm of formic acid, 25.32 ppm of acetic acid, 72.67 ppm of acetone, 39.93 ppm of methanol, 5.32 ppm of 1,2-Isobutenediol, 74.88 ppm of isopropyl alcohol, 57.51 ppm of ethanol, 5.01 ppm of 1-Hidroxy-2-propanone, 92.36 ppm of 1-Propanol, 5.35 ppm of 2,4-Pentadione, 42.67 ppm of 3-Methyl-2-pentanol and 92.36 ppm of 1-Butanol in He balance.

Table 1
Characterization of samples of interest.

	PP0	PP1	PP2	PP3	PP4	PP5	PP6	PP7	PP8	PP9	PP10
As, mg Kg^{-1}	0.001	0.05	0.12	0.23	0.42	0.77	1.18	2.19	3.34	3.84	4.32
Moisture, wt%	0.18	0.33	0.21	0.18	0.22	0.35	0.18	0.18	0.18	0.18	0.18
MFI	3.00	3.11	3.86	4.23	5.10	7.11	9.11	14.61	20.21	21.47	24.51
Ti, ppm	0.98	0.98	0.98	0.98	0.98	0.98	0.98	0.98	0.98	0.98	0.98
Al, ppm	8.55	8.25	8.64	8.41	8.09	8.19	8.31	8.52	8.32	8.15	8.57
Cl, ppm	12.25	12.35	12.45	12.08	13.04	12.86	13.54	13.08	13.25	13.64	13.52
Fe, ppm	4.25	4.74	4.65	4.72	4.61	4.44	4.09	4.35	4.82	4.56	4.44
Correlation MFI Vs As, mg Kg^{-1}	Y= 4.7569X + 3.111. R2 = 0.9993										

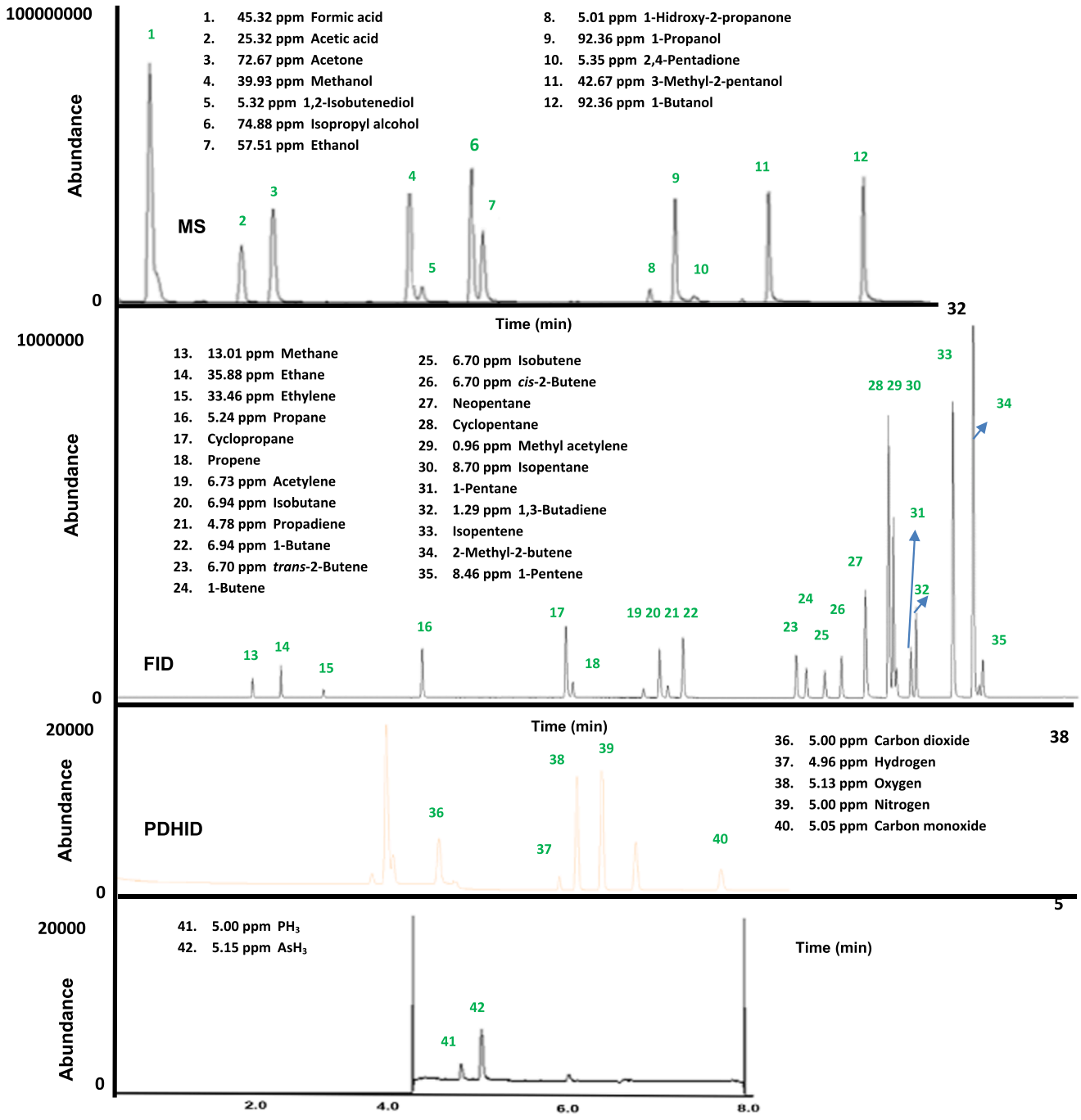

Fig. 2. Simultaneous chromatograms of oxygenates, permanent gases, hydrocarbons and arsine.

2.1.1. Preparation of the calibration curve for AsH_3

AsH_3 standards were used with concentration ranges of 0.1, 0.5, 1.0 and 3.0 ppm in Liquefied petroleum gas (LPG) balance.

2.2. Preparation of PP samples with different concentrations of AsH_3

The 11 virgin-PP (PP0 to PP10) samples were obtained during the polymerization process using a ZN catalyst. Fig. 1 shows a summary of the polymerization stage. 4 sampling points were identified. Each point was sampled 10 times. Point A corresponds to refinery grade propylene monomer. Point B, corresponds to propylene recovered after the polymerization reaction. Point C, propylene gases inside the reactor and Point D, synthesized virgin-PP desorption gases. The AsH_3 is injected through the bottom of the reactor. During the synthesis of PP, varied flows of AsH_3 were injected to ensure that the 11 samples of PP presented different levels of AsH_3 and arsenic. Table 1 shows the final concentration of AsH_3 and arsenic in LPG and the matrix of each PP respectively. The 11 virgin-PP samples were taken at point E of Fig. 1.

2.3. Apparatus and procedure

2.3.1. Thermogravimetric analyzer (TGA)

TGA was performed on a Perkin Elmer TGA7 thermogravimetric analyzer at a heating rate of 20 °C min^{-1} with a scan range from room temperature to 600 °C. In each test, a 10 mg sample was examined under N_2 with a flowing rate of 60 mL min^{-1} [52]. With the TG and DTG curves, all the thermal degradation data was obtained [59,60].

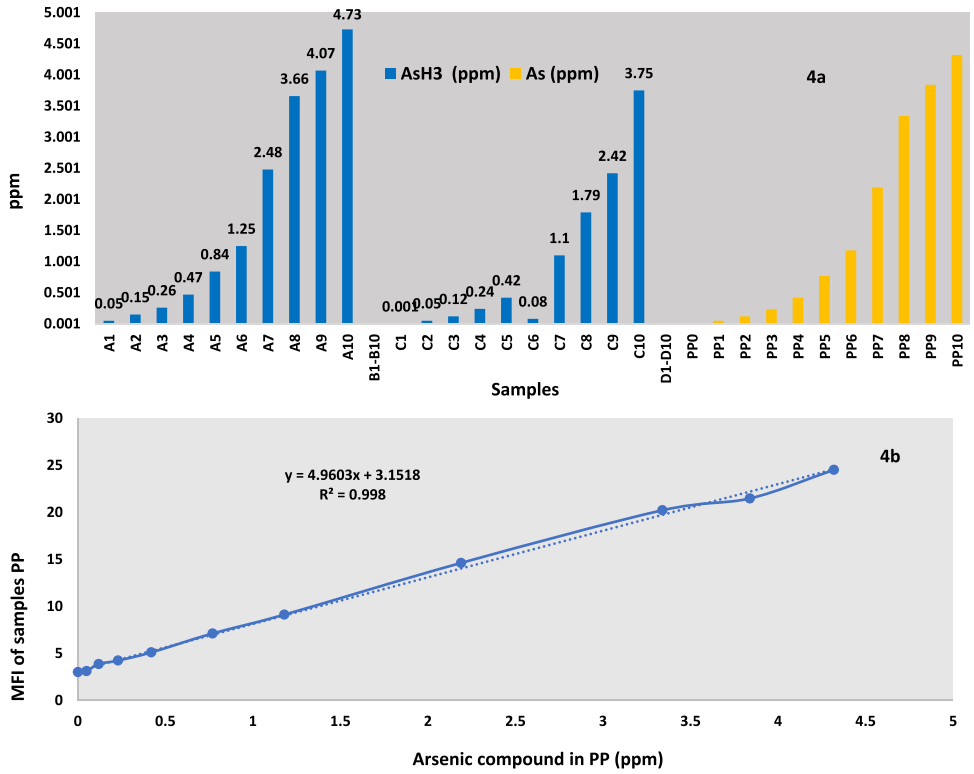

Fig. 3. (3a) Concentration of AsH_3 and As in the PP polymerization process and in PP. (3b) Correlation between the concentration of Arsenic compounds in PP and MFI.

2.3.2. *X-ray fluorescence*

The qualitative and quantitative elementary analysis of arsenic was made with a Malvern Panalitycal Axios FAST.

2.3.3. *Melt flow index (MFI)*

MFI of the different PP samples was carried out in a Tinius Olsen MP1200 plastometer. The temperature inside the plastometer cylinder was 230 °C and a 2.16 kg piston was used to displace the melt. MFI values were used to evaluate the average molecular weight for each formulation by using the Bremner approximation, as indicated in the following equation.

$$M_w^{3,7} = \frac{1.675}{(MFI230°C.2.16kg) \quad X \quad 10^{-21}}$$

2.3.4. *Fourier transform infrared (FT-IR)*

FT-IR was carried out using a Nicolet Magna-IR 830 spectrometer using the attenuated total reflectance method (ATR).

2.3.5. *Pyrolysis and thermo-degradation*

This experimentation was carried out using a quartz pyrolizer, the reactor placed in a horizontal tubular oven and an oven with selective temperature control. For the tests ± 20 g of each PP were weighed, the working temperature was constant at 500 °C, and N_2 of 99.999% purity was used with a flow of 100 mL min^{-1} [52]. At the start of the experiment, 10 g of PP was loaded into the reactor, which was then heated to 120 °C at 5 °C min^{-1} and held for 1 h to remove any moisture and oxygen from the reactor. Once the pyrolysis was finished, the solid carbonaceous residues present inside the quartz reactor were removed and discarded. The gas products obtained from the pyrolysis of PP0 and waste PP10 were collected in a duly deactivated stainless steel cylinders, with a capacity of 200 mL and includes a relief valve. The gases were transported to the injection port of the chromatograph.

An Agilent technologies 7890B gas chromatograph was used for the analysis of oxygenates, hydrocarbons, arsine and permanent compounds in gas samples from the pyrolizer. The GC has two Agilent 5977 MS detectors, one FID detector and one PDHID detector. The MS detectors have electron impact ionization sources at 230 °C, and a transfer line at 280 °C. GC has 7 Vs (valves):Vs 4 (0.11 on and 0.6 off), Vs 5 (on), Vs 2 (1.45 on and 3.0 off),Vs 3 (0.11 on and 1.8 off), Vs 7 (0.15 on and 0.7 off) and 8 (1.6 on and 5.1 off)). 9 columns: R (HP-1, 3 m × 0.1 mm), 1 (DB-1, 100% Dimethylpolyxilosane, 60 m × 320 μm × 0.25 μm), 3 (HP-PLOT MoleSieve, 15 m × 0.53 mm × 50 μm), 4 (GS-Al/KCl 50 m × 0.53 mm), 5 (HP-PLOT Q, 15 m × 0.53 mm×40 μm), 6 (HP-PLOT MoleSieve, 30 m × 0.53 mm × 50 μm), 7a (HP-PLOT Q, 15 m x 0.53 mm×40 μm) and column 7b (HP-PLOT Q, 15 m x 0.53 mm×50 μm)) [61–63]. The oven temperature starts at 40 °C × 3 min, increasing to 60 °C a 10 °C min^{-1} × 4 min and finally, increasing to 170–35 °C min^{-1} for 25 min Fig. 2 shows the chromatograms of the standards for AsH_3, oxygenates, hydrocarbons and permanent gases.

3. Results and discussion

3.1. *Preparation of PP samples with different concentrations of AsH_3*

3.1.1. *Quantification of AsH_3 in the PP polymerization stage and demonstration of the stage where its absorption in the PP matrix takes place*

Fig. 3a shows that the concentration of AsH_3 at sampling points A1 to A10 varies between 0.05 and 4.73 ppm. The percentage difference between the maximum and minimum values was 99%. Intermediate samples between A1 and A10 showed significant percentage increases in AsH_3. These results indicate that samples at these points are a potential source of AsH_3. Its presence at this sampling points is the product of deficiencies in the purification stages in the petrochemical plants that supply this refinery grade propylene. Sampling point B, which corresponds to the recovered propylene, was sampled and analyzed. At this point the presence of AsH_3 is not evident. These results indicate that all AsH_3 present in the refinery grade propylene and entering the reactor is absorbed or adsorbed into the virgin-PP being synthesized. Point C

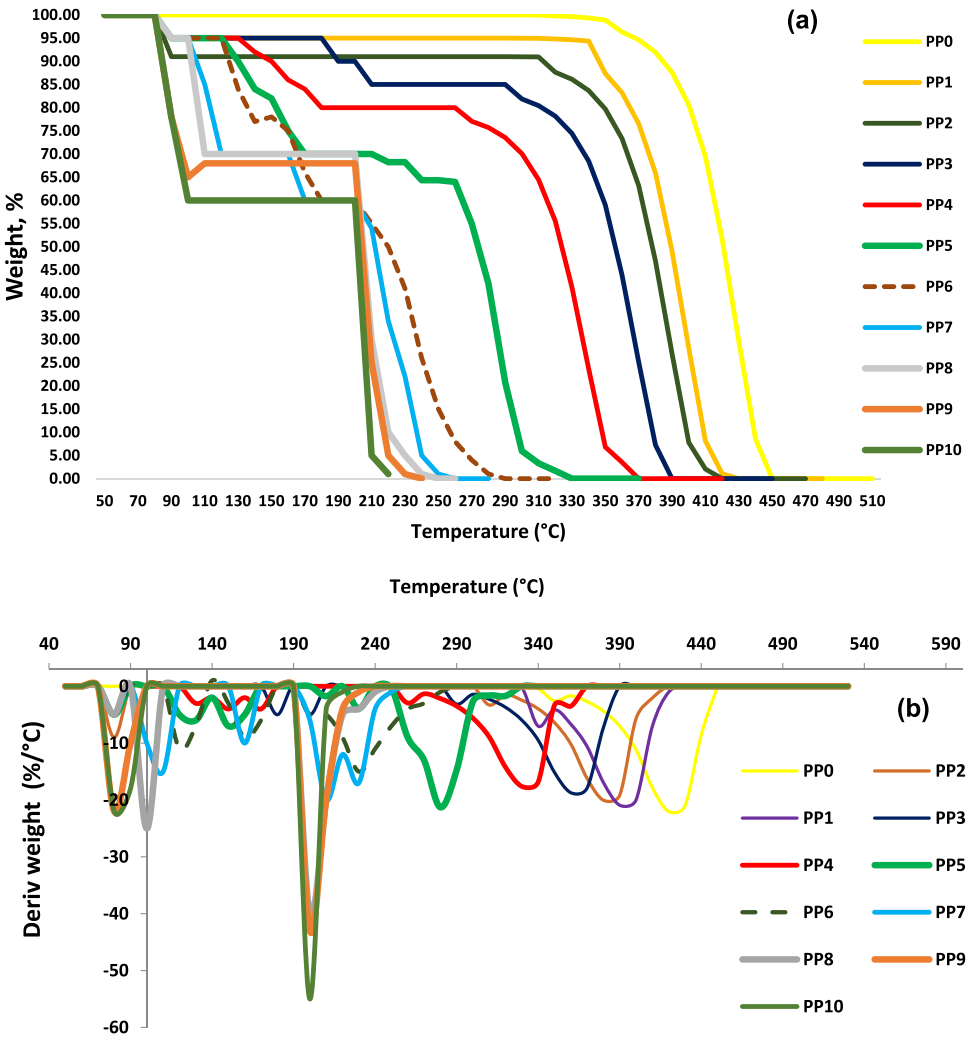

Fig. 4. TG(a) and DTG(b) curves of the 11 PP samples.

corresponds to the gaseous propylene inside the polymerization reactor. At this point the maximum and minimum concentrations of AsH_3 between C1 and C10 were 0.001 and 3.75 ppm, indicating that before the start of polymerization there are traces of AsH_3, but as the reaction progresses or when the ZN catalyst dosing rate is increased, the ppm of AsH_3 decrease to a value of zero. This is confirmed, since at point B, the concentration of AsH_3 is zero. Point D corresponds to a desorption column where water steam and N_2 are injected into the virgin-PP, to remove all volatile compounds, which are adsorbed into the polymer matrix. The gaseous sample was sampled and analyzed, showing the absence of AsH_3, which allows us to conclude that this AsH_3 is not adsorbed in the matrix of the virgin-PP, and that there is a high probability that it is absorbed and forms a stable compound. The monitored process also indicates that the final virgin-PP presented different levels of concentration of Arsenic compounds, because propylene with varied concentration of AsH_3 enters during its synthesis, as evidenced at sampling point A. Therefore, the virgin-PP obtained and sampled at point E is considered a product that is out of specifications and therefore solid waste. It is characterized as industrial waste, meaning that because this virgin-PP is an industrial waste it must have properties different from a virgin-PP free of AsH_3.

3.2. Quantification of arsenic in virgin-PP samples and determination of its effects on MFI

Table 1 and Fig. 3b shows significant differences in Arsenic content in three of 11 virgin-PP industrial samples. Arsenic concentrations do not have significant estechiometric differences when compared to the Arsenic content present in the AsH_3 molecule, demonstrating that the source of Arsenic is from AsH_3 impurities as observed in the concentrations at sampling point A. These results tell us that AsH_3 must react with the ZN catalyst to form a complex that remains stable in the virgin-PP matrix. The lowest values of MFI (3.00 and 3.11 ppm) and Arsenic (0.001 and 0.05 ppm) are observed in samples PP0 and PP1, while the highest values of MFI (21.47 and 24.51) and Arsenic (4.1 and 4.87) are seen in samples PP9 and PP10. These results tell us that there should be a reaction mechanism where AsH_3 competes with the propylene molecule from the polymerization stage, and that AsH_3 is the one with the highest speed, reacting with the active center of the ZN and affecting the growth of the polymer chain. Table 1 lets you see there is a linear correlation between MFI and Arsenic and AsH_3 concentration, with an R^2 of 0.9993. This indicates that, for these industrial wastes of virgin-PP, its MFI increases when the concentration of AsH_3 in the refinery grade propylene increases, thus showing the existence of a high reactivity by the ZN catalyst. Therefore, chain scissions and polymer structure fractures into smaller macromolecules during degradation are common, resulting in decreasing the average molecular weight and by the increase in the MFI. The 11 samples did not show significant differences in the residue content of Ti, Al, Cl and Fe catalysts, displaying in this way that changes in MFI and PP stability are not generated by these residuals, as if it has been demonstrated in other research [52].

Table 2
Compounds identified and quantified in pyrolysis with N_2.

Composts	SAMPLES										
	PP0	PP1	PP2	PP3	PP4	PP5	PP6	PP7	PP8	PP9	PP10
ALKANS											
Methane, % mol	5,5	2,1	1,5	0,8	0,5	0,4	0,3	0	0	0	0
Ethane, % mol	12,8	7,2	5	4,5	4,2	3,5	3	0	0	0	0
Propane, % mol	3,7	2,1	3,4	3	2,5	2,2	1,5	0	0	0	0
Cyclopropane, % mol	0,05	0	0	0	0	0	0	0	0	0	0
Isobutane, % mol	0,6	0	0	0	0	0	0	0	0	0	0
N- Butane, % mol	1,7	1,4	0,5	0,3	0,2	0,1	0	0	0	0	0
Isopentane, % mol	10,8	5,2	4,7	4,2	3,7	3,1	2,1	0	0	0	0
Total Amount	**35,15**	**18**	**15,1**	**12,8**	**11,1**	**9,3**	**6,9**	**0**	**0**	**0**	**0**
ALKENES											
Ethylene, % mol	1,8	1	1	0,7	0,5	0,4	0,1	0	0	0	0
Propylene, % mol	59,4	44,4	34	29	22	17	10	8	1	0	0
Propadiene, % mol	0,4	0,4	0,4	0,2	0,1	0,1	0,1	0,1	0,1	0	0
Trans-2-Butene, % mol	0,3	0,3	0,4	0,3	0,2	0,1	0,1	0,1	0,1	0	0
1-Butene, % mol	0,2	0,2	0,6	0,4	0,3	0,1	0,1	0,1	0,1	0	0
Cis-2-Butene, % mol	0,1	0,1	0,7	0,4	0,2	0,1	0,1	0,1	0,1	0	0
1,3- Butadiene, % mol	0,1	0,1	0,5	0,1	0	0	0	0	0	0	0
1-Pentene, % mol	0,1	0,1	0,5	0,4	0,2	0,2	0	0	0	0	0
Total Amount	**62,4**	**46,6**	**38,1**	**31,5**	**23,5**	**18**	**10,5**	**8,4**	**1,4**	**0**	**0**
ALKYNES											
Acetylene, % mol	0,1	1,2	1,6	2,1	2,6	3,2	3,7	4,1	4,7	3,5	1,4
Methyl acetylene, % mol	0,2	1,5	2,1	2,7	3,5	3,3	3,9	4,5	4,9	3,1	1,1
Total Amount	**0,3**	**2,7**	**3,7**	**4,8**	**6,1**	**6,5**	**7,6**	**8,6**	**9,6**	**6,6**	**2,5**
ALCOHOL											
Methanol, % mol	0,1	2,5	3,9	4,2	4,7	5,1	5,4	5,9	6,2	6,5	6,4
Ethanol, % mol	0,1	2,1	2,5	3,1	3,8	4,4	4,9	5,5	5,9	6,2	6,5
Alcohol isopropyl, % mol	0,01	2,1	2,8	3,3	3,9	4,3	5,2	6,1	6,5	6,9	7,2
N-Propanol, % mol	0,02	1,4	1,9	2,4	2,9	3,5	4,4	4,9	5,2	5,5	5,7
N-Butyl Alcohol, % mol	0	1,4	1,7	2,2	3,2	3,7	4,3	4,9	5,4	5,8	6
1,2- Isobutenediol, % mol	0	1,4	1,8	2,2	2,9	3,2	3,9	4,3	4,9	5,2	5,5
3-Methyl-2-Pentanol, % mol	0	2,4	2,7	3,4	4,2	4,7	5,4	5,9	6,3	6,7	6,9
Total Amount	**0,23**	**13,3**	**17,3**	**20,8**	**25,6**	**28,9**	**33,5**	**37,5**	**40,4**	**42,8**	**44,2**
KETONE											
Acetone, % mol	0,1	3	4,1	4,8	5,1	5,6	6,4	7,7	8,2	8,5	9
1-Hydroxy-2-Propanone, % mol	0,02	3,2	3,5	4,4	4,9	5,4	5,6	6,4	6,7	7,1	7,5
2,4-Pentadione, % mol	0,01	3	3,8	4,3	4,9	5,3	6,2	6,7	7,1	7,4	7,6
2-Pentanone, % mol	0,1	3,1	3,9	4,4	4,8	5,4	5,9	6,5	6,9	7,3	7,5
Total Amount	**0,23**	**12,3**	**15,3**	**17,9**	**19,7**	**21,7**	**24,1**	**27,3**	**28,9**	**30,3**	**31,6**
ACIDS											
Formic Acid, % mol	0,1	2,1	3,3	3,9	4,3	4,8	5,3	6,2	6,8	7,2	7,5
Acetic Acid, % mol	0,2	2,3	3,4	4	4,5	5,1	5,5	6,4	6,7	7,1	7,4
Total Amount	**0,3**	**4,4**	**6,7**	**7,9**	**8,8**	**9,9**	**10,8**	**12,6**	**13,5**	**14,3**	**14,9**
PERMANENTS											
CO, % mol	0,1	0,5	0,7	0,9	1,2	1,4	1,4	0,1	0,15	0,1	0,2
CO_2, % mol	0,5	1,1	1,7	2,2	2,4	2,7	3,4	3,8	4,1	4,4	4,5
O_2, % mol	0,1	0,2	0,2	0,3	0,4	0,4	0,6	0,6	0,7	0,7	0,7
H_2, % mol	0,8	0,9	1,2	0,9	1,2	1,2	1,2	1,1	1,3	1,2	1,4
Total Amount	**1,5**	**2,7**	**3,8**	**4,3**	**5,2**	**5,7**	**6,6**	**5,6**	**6,25**	**6,4**	**6,8**
ARSINE											
AsH_3, % mol	0	0	0	0	0	0	0	0	0	0	0
Total Amount	0	0	0	0	0	0	0	0	0	0	0

3.3. Residual impact of arsenic on the degradation of PP

In Fig. 4, shows TG(a) and DTG(b) for the samples PP0 to PP10. The samples have been analyzed with one and four break down peak at different temperature. The sample PP0 have a thermal behavior in compare with the literature at 20 °C min^{-1} [19]. PP0 and PP1, shows the smaller value for arsenic in his polymeric matrix and a one break down peak at 390 and 420 °C with a mass loss for 22% ° C^{-1}. The sample PP2 shows two breaks down peak, one of them at 80 °C and the other at 380 °C, with a mass loss for 9% and 20%° C^{-1} respectively. Every sample shows significant increase in the arsenic's concentration, with a decrease in the PP thermal stability, as show by PP3, PP7, PP8 and PP10, where each of them have 4 breaks down peak, being PP3 with more stability, because the thermal decomposition is between 190 and 380 °C. the remaining samples PP, PP8 and PP10, shows an important mass loss at temperature under 100 °C, while at 200 °C shows mass loss between 20% and 55%° C^{-1}. The biggest mass loss shows the samples PP10, in addition show a lost for 22, 18, 40%° C^{-1} in a at range temperature between 80 and 90 °C respectively. The previous perform is not commonly in the polymeric chain for the PP and point in the macromolecular structure have significant changes, results for the AsH_3 addition in the polymerization stage for each of them PPs, generate molecular extracts with low molar weight, low thermal stability, in presence to functional groups different from the hydrocarbon. This phenomenon enables a high relevance for the propose about new reaction mechanism, let interpret the AsH_3 reactions with ZN catalyst, and explain the reduce in the physicochemical properties for the PPs. The TG and DTG of each sample PP4, PP5, PP6 and PP9 include 3 peaks with break down temperature on average 80,100–170 and 200–360 °C. For this samples, the biggest range in loss mass ranges between 18% and 43% ° C^{-1} for PP4 and PP9. Is important to show, PP9 have the most arsenic concentration and set out mass loss for 22 CE 10% ° C^{-1} at 80 y 90 °C.

Table 3
Compounds identified and quantified in thermo-oxidative degradation.

Composts	SAMPLES										
	PP0	PP1	PP2	PP3	PP4	PP5	PP6	PP7	PP8	PP9	PP10
ALKANS											
Methane, % mol	1,2	0	0	0	0	0	0	0	0	0	0
Ethane, % mol	3,5	0	0	0	0	0	0	0	0	0	0
Propane, % mol	1,7	0	0	0	0	0	0	0	0	0	0
Cyclopropane, % mol	0,01	0	0	0	0	0	0	0	0	0	0
Isobutane, % mol	0,1	0	0	0	0	0	0	0	0	0	0
N- Butane, % mol	0,02	0	0	0	0	0	0	0	0	0	0
Isopentane, % mol	0,1	0	0	0	0	0	0	0	0	0	0
Total Amount	**6,63**	**0**	**0**	**0**	**0**	**0**	**0**	**0**	**0**	**0**	**0**
ALKENES											
Ethylene, % mol	0,5	0	0	0	0	0	0	0	0	0	0
Propylene, % mol	5,6	0	0	0	0	0	0	0	0	0	0
Propadiene, % mol	0,01	0	0	0	0	0	0	0	0	0	0
Trans-2-Butene, % mol	0,05	0	0	0	0	0	0	0	0	0	0
1-Butene, % mol	0,1	0	0	0	0	0	0	0	0	0	0
Cis-2-Butene, % mol	0,08	0	0	0	0	0	0	0	0	0	0
1,3- Butadiene, % mol	0,07	0	0	0	0	0	0	0	0	0	0
1-Pentene, % mol	0,1	0	0	0	0	0	0	0	0	0	0
Total Amount	**6,51**	**0**	**0**	**0**	**0**	**0**	**0**	**0**	**0**	**0**	**0**
ALKYNES											
Acetylene, % mol	0,05	0	0	0	0	0	0	0	0	0	0
Methyl acetylene, % mol	0,04	0	0	0	0	0	0	0	0	0	0
Total Amount	**0,09**	**0**	**0**	**0**	**0**	**0**	**0**	**0**	**0**	**0**	**0**
ALCOHOL											
Methanol, % mol	0,5	0	0	0	0	0	0	0	0	0	0
Ethanol, % mol	0,4	0	0	0	0	0	0	0	0	0	0
Alcohol isopropyl, % mol	0,1	0	0	0	0	0	0	0	0	0	0
N-Propanol, % mol	1,5	0	0	0	0	0	0	0	0	0	0
N-Butyl Alcohol, % mol	2,1	0	0	0	0	0	0	0	0	0	0
1,2- Isobutenediol, % mol	2	0	0	0	0	0	0	0	0	0	0
3-Methyl-2-Pentanol, % mol	3,1	0	0	0	0	0	0	0	0	0	0
Total Amount	**9,7**	**0**	**0**	**0**	**0**	**0**	**0**	**0**	**0**	**0**	**0**
KETONE											
Acetone, % mol	0,2	0,8	1,4	0	0	0	0	0	0	0	0
1-Hydroxy-2-Propanone, % mol	0,5	1,4	2,4	0	0	0	0	0	0	0	0
2,4-Pentadione, % mol	0,3	5	0,4	0	0	0	0	0	0	0	0
2-Pentanone, % mol	0,2	4,2	0,7	0	0	0	0	0	0	0	0
Total Amount	**1,2**	**11,4**	**4,9**	**0**	**0**	**0**	**0**	**0**	**0**	**0**	**0**
ACIDS											
Formic Acid, % mol	7,1	6,2	7	5,1	2,2	0	0	0	0	0	0
Acetic Acid, % mol	8,2	7,2	8,1	7,1	2,7	0	0	0	0	0	0
Total Amount	**15,3**	**13,4**	**15,1**	**12,2**	**4,9**	**0**	**0**	**0**	**0**	**0**	**0**
PERMANENTS											
CO, % mol	7,07	0	0	0	0	0	0	0	0	0	0
CO_2, % mol	50	75,2	80	87,8	93,3	100	100	100	100	100	100
O_2, % mol	0,1	0	0	0	0	0	0	0	0	0	0
H_2, % mol	3,2	0	0	0	0	0	0	0	0	0	0
Total Amount	**60,37**	**75,2**	**80**	**87,8**	**93,3**	**100**	**100**	**100**	**100**	**100**	**100**

3.4. Characterization of gases formed during thermo-oxidation and pyrolysis of PP samples

The 11 samples of interest were pyrolyzed and the behavior of the data is shown in Table 2. The highest percentage of alkenes was found in PP0 with an average value of 62.4%, and the lowest values were quantified in samples PP8, PP9 and PP10, where values ranged from 0% to 1.4%. The total concentrations of alcohols, ketones, carboxylic acids, and permanent gases, increased with the arsenic content in the matrix of samples of interest, and this is seen in Table 2 where PP0 to PP10 had total concentrations of oxidized species of 2.26%, 32.7%, 43.1%, 50.9%, 59.3%, 66.2%, 75.0%, 83.0%, 89.1% and 97.5%, respectively. In the pyrolysis process the alcohols were the groups identified at the highest concentration, followed by ketones, carboxylic acids and, finally, permanent gases. PP0 shows an alcohol content of 0.23%, 0.23% ketones, 0.3% acids and 1.5% permanent gases. Samples PP8, PP9 and PP10 had a higher fluidity rate and higher arsenic content and the highest average concentrations of alcohols, ketones, acids, and permanent gases of 42.5%, 30.3%, 14.2% and 6.5%. This shows that the higher levels of degradation are produced by the highest concentrations of AsH_3 in propylene, and the highest values of arsenic in the matrix of industrial waste of PP. Table 2 and Table 3 show the qualitative and quantitative results of all the chemical species present in the gases produced during the thermo-degradation and pyrolysis of the 11 PP samples.

Table 3 show the results of thermo-degradation for the 11 samples of interest. Samples from PP0 to PP10 did not show the presence of alkanes, alkenes, alkynes and alcohol functional groups. Ketones and carboxylic acids were only identified in PP0, PP1, PP2, PP3, PP4 and PP5. Permanent gases were present in all samples and with increasing concentrations from PP0 to PP5. From PP5 to PP10 CO_2 concentrations were of 100%, indicating complete oxidation and related to identified thermal stability and high concentrations of arsenic in the matrix, which will increase the rate of degradation of these samples, as the result of increased free radical formation and oxygenated species.

4. Conclusions

The effect of AsH_3 concentrations on the degradation rate of virgin-PP residues is very high and increases significantly as it transitions from an atmosphere in N_2 to one with O_2, reducing the hydrocarbon and

oxygenated content and increasing CO_2 by 100% especially for those residues with higher arsenic content in its matrix. During pyrolysis, the highest percentage of alkanes was found in PP0 with an average value of 62.4%, and the lowest values in PP8, PP9 and PP10 with oscillations between 0% and 1.4%. The total concentration of oxidized species for PP0 to PP10 was 2.26%, 32.7%, 43.1%, 50.9%, 59.3%, 66.2%, 75.0%, 83.0%, 89.1% and 97.5% respectively.

CRediT authorship contribution statement

The author thanks Esenttia for the space to carry out this research.

Declaration of Competing Interest

The authors declare that they have no known competing financial interests or personal relationships that could have appeared to influence the work reported in this paper.

References

[1] J. Hernández-Fernández, J. López, Quantification of poisons for Ziegler Natta catalysts and effects on the production of polypropylene by gas chromatographic with simultaneous detection: Pulsed discharge helium ionization, mass spectrometry and flame ionization, J. Chromatogr. A 2020 (1614) 460736–460743.
[2] R. Gras, J. Luong, M. Hawryluk, M. Monagle, Analysis of part-per-billion level of arsine and phosphine in light hydrocarbons by capillary flow technology and dielectric barrier discharge detector, J. Chromatogr. A 1217 (2010) 348–352.
[3] G. Wilkinson, R.D. Gillard, J.A. McCleverty (Eds.), Comprehensive Coordination Chemistry, Pergamon Press, Oxford, 1987.
[4] J.A. McCleverty, T.J. Meyer (Eds.), Comprehensive Coordination Chemistry II, Elsevier, Oxford, 2004.
[5] C.A. McAuliffe, W. Levason, Phosphine, Arsine and Stibine Complexes of the Transition Elements, Elsevier, Amsterdam, 1979.
[6] (a) P.W.N.M. van Leeuwen, Homogeneous Catalysis Understanding the Art, Kluwer Academic Publishers, Dordrecht, 2004;
(b) R.H. Crabtree, The Organometallic Chemistry of the Transition Metals, fourth ed., John Wiley & Sons,, 2005.
[7] W. Levason, G. Reid, Developments in the coordination chemistry of stibine ligands, Coord. Chem. Rev 250 (2006) 2565–2594.
[8] A.G. Orpen, N.G. Connelly, Structural systematics: the role of P-A.sigma.* orbitals in metal-phosphorus.pi.-bonding in redox-related pairs of M-PA3 complexes (A = R, Ar, OR; R = alkyl, Organometallics 9 (1990) 1206–1210.
[9] L. Cavallo, S. Del Piero, J.-M. Ducéré, R. Fedele, A. Melchior, G. Morini, F. Piemontesi, M. Tolazzi, Key interactions in heterogeneous Ziegler−Natta catalytic systems: structure and energetics of TiCl4−Lewis base complexes, J. Phys. Chem. C 111 (2007) 4412–4419.
[10] N. Bahri-Laleh, M. Nekoomanesh-Haghighi, S.A. Mirmohammadi, A DFT study on the effect of hydrogen in ethylene and propylene polymerization using a Ti-based heterogeneous Ziegler–Natta catalyst, J. Organomet. Chem. 719 (2012) 74–79.
[11] A. Correa, N. Bahri-Laleh, L. Cavallo, How well can DFT reproduce key interactions in Ziegler–Natta systems, Macromol. Chem. Phys. 214 (2013) 1980–1989.
[12] V. Nikolaevna Panchenko, L. Viktorovna Vorontsova, V. Aleksandrovich Zakharov, Ziegler-Natta catalysts for propylene polymerization – interaction of an external donor with the catalyst, Polyolefins J. 4 (2017) 87–97.
[13] M. Nikolaeva, T. Mikenas, M. Matsko, V. Zakharov, Effect of AlEt3 and an external donor on the distribution of active sites according to their stereospecificity in propylene polymerization over TiCl4/MgCl2 catalysts with different titanium content, Macromol. Chem. Phys. 217 (2016) 1384–1395.
[14] E.I. Vizen, L.A. Rishina, L.N. Sosnovskaja, F.S. Dyachkovsky, I.L. Dubnikova, T. A. Ladygina, Study of hydrogen effect in propylene polymerization on (with) the MgCl2 supported Ziegler-natta catalyst- part 2. Effect of CS2 on polymerization centres, Eur. Polym. J. 30 (1994) 1315–1318.
[15] K. Kallio, A. Wartmann, K.H. Reichert, Reactivation of a poisoned metallocene catalyst by irradiation with visible light, Macromol. Rapid Commun. 23 (2002) 187–190.
[16] N. Bahri-Laleh, Interaction of different poisons with MgCl2/TiCl4 based Ziegler-Natta catalysts, Appl. Surf. Sci. 379 (2016) 395–401.
[17] S. Pasynkiewicz, Reactions of organoaluminium compounds with electron donors, Pure Appl. Chem. 30 (1972) 509–522.
[18] J. Hernandez-Fernandez, Quantification of oxygenates, sulphides, thiols and permanent gases in propylene. A multiple linear regression model to predict the loss of efficiency in Polypropylene production on an industrial scale, J. Chromatogr. A 2020 (1628) 461478–461489.
[19] R.J.H. Clark, in: J.C. Bailar, H.J. Emeleus, R.S. Nyholm, A.F. Trotman-Dickenson (Eds.), Comprehensive Inorganic Chemistry, vol. 3, Pergamon, Oxford, 1973. Ch. 3.
[20] C.A. McAuliffe, D.S. Barratt, in: G. Wilkinson, R.D. Gillard, J.A. McCleverty (Eds.), Comprehensive Coordination Chemistry I, vol. 3, Pergamon, Oxford, 1987 (Ch. 31).
[21] M.R. Jan, J. Shah, H. Gulab, Catalytic degradation of waste high-density polyethylene into fuel products using BaCO3 as a catalyst, Fuel Process. Technol. 91 (11) (2010) 1428–1437.
[22] M. Seifali Abbas-Abadi, M. Nekoomanesh Haghighi, H. Yeganeh, The effect of temperature, catalyst, different carrier gases and stirrer on the produced transportation hydrocarbons of LLDPE degradation in a stirred reactor, J. Anal. Appl. Pyrolysis 95 (2012) 198–204.
[23] M. Seifali Abbas-Abadi, M. Nekoomanesh Haghighi, H. Yeganeh, Evaluation of pyrolysis product of virgin high density polyethylene degradation using different process parameters in a stirred reactor, Fuel Process. Technol. 109 (2012) 90–95.
[24] A. Marcilla, M.I. Beltrán, R. Navarro, Thermal and catalytic pyrolysis of polyethylene over HZSM5 and HUSY zeolites in a batch reactor under dynamic conditions, Appl. Catal. B: Environ. 86 (2009) 78–86.
[25] E. Ahmad, S. Chadar, S.S. Tomar, M.K. Akram, Catalytic degradation of waste plastic into fuel oil, Int. J. Petrol. Sci. Technol. 3 (1) (2009) 25–34.
[26] S.H. Jung, M.H. Cho, B.S. Kang, J.S. Kim, Pyrolysis of a fraction of waste polypropylene and polyethylene for the recovery of BTX aromatics using a fluidized bed reactor, Fuel Process. Technol. 91 (2010) 277–284.
[27] M. Salman, R. Rehman, U. Shafique, T. Mahmud, B. Ali, Comparative thermal and catalytic recycling of low density polyethylene into diesel-like oil using different commercial catalysts, Electron. J. Environ. Agric. Food Chem. 11 (2) (2012) 96–105.
[28] M.N. Almustapha, J.M. Andrésen, Recovery of valuable chemicals from high density polyethylene (HDPE) polymer: a catalytic approach for plastic waste recycling, Int. J. Environ. Sci. Dev. 3 (2012) 3–267.
[29] D.C. Tiwari, E. Ahmad, K.K. Kumar Singh, Catalytic degradation of waste plastic into fuel range hydrocarbons, Int. J. Chem. Res. 1 (2) (2009) 31–36.
[30] M.F. Ali, M.S. Qureshi, Catalyzed pyrolysis of plastics: a thermogravimetric study, Afr, J. Pure Appl. Chem. 5 (9) (2011) 284–292.
[31] G. De la Puente, C. Klocker, U. Sedran, Conversion of waste plastics into fuels recycling polyethylene in FCC, Appl. Catal. B: Environ. 36 (2002) 279–285.
[32] K.H. Lee, Composition of aromatic products in the catalytic degradation of the mixture of waste polystyrene and high-density polyethylene using spent FCC catalyst, Polym. Degrad. Stab. 93 (2008) 1284–1289.
[33] S.L. Wong, N. Ngadi, T.A.T. Abdullah, I.M. Inuwa, Conversion of low density polyethylene (LDPE) over ZSM-5 zeolite to liquid fuel, Fuel 192 (2017) 71–82.
[34] R. Miandad, M.A. Barakat, A.S. Aburiazaiza, M. Rehan, A.S. Nizami, Catalytic pyrolysis of plastic waste: a review, Process Saf. Environ. Prot. 102 (2016) 822–838.
[35] Y. Sakata, M.A. Uddin, A. Muto, Degradation of polyethylene and polypropylene into fuel oil by using solid acid and non-acid catalysts, J. Anal. Appl. Pyrolysis 51 (1999) 135–155.
[36] S. Thornberg, R. Bernstein, A. Irwin, D. Derzon, S. Klamo, R. Clough, The genesis of CO_2 and CO in the thermooxidative degradation of polypropylene, Polym. Degrad. Stab. 92 (2007) 94–102.
[37] R. Bernstein, S. Thornberg, R. Assink, A. Irwin, J. Hochrein, J. Brown, D. Derzon, S. Klamo, R. Clough, The origins of volatile oxidation products in the thermal degradation of polypropylene, identified by selective isotopic labeling, Polym. Degrad. Stab. 92 (2007) 2076–2094.
[38] J. Chien, C. Boss, Polymer reactions. V. Kinetics of autoxidation of polypropylene, J. Polym. Sci.,Part A: Polym. Chem. 5 (1967), 309-101.
[39] J. Chien, C. Boss, Polymer reactions. VI. Inhibited autoxidation of polypropylene, J. Polym. Sci.,Part A: Polym. Chem. 5 (1967) 1683–1697.
[40] J. Chien, E. Vandenberg, H. Jabloner, Polymer reactions. III. Structure of polypropylene hydroperoxide, J. Polym. Sci.,Part A: Polym. Chem. 6 (1968) 381–392.
[41] D. Carlsson, D. Wiles, The photodegradation of polypropylene fiof pol. Photolysis of ketonic oxidation products, Macromolecules 2 (1969) 587–597.
[42] D. Carlsson, D. Wiles, The photodegradation of polypropylene films.III. Photolysis of polypropylene hydroperoxides, Macromolecules 2 (1969) 597–606.
[43] J. Adams, Analysis of the nonvolatile oxidation products of polypropyl-ene I. Thermal oxidation, J. Polym. Sci.,Part A: Polym. Chem. 8 (1970) 1077–1090.
[44] J. Adams, Analysis of the nonvolatile oxidation products of polypropyl-ene II. Process degradation, J. Polym. Sci.,Part A: Polym. Chem. 8 (1970) 1269–1277.
[45] J. Adams, Analysis of the nonvolatile oxidation products of polypropyl-ene III. Photodegradation, J. Polym. Sci. Part A: Polym. Chem. 8 (1970) 1279–1288.
[46] C. Decker, F. Mayo, Aging and degradation of polyolefins. II.ϒ-Initiatedoxidations of atactic polypropylene, J. Polym. Sci. Part A: Polym. Chem. 11 (1973) 2847–2877.
[47] E. Niki, C. Decker, F. Mayo, Aging and degradation of polyolefins. I.Peroxide-initiated oxidations of atactic polypropylene, J. Polym. Sci. Part A: Polym. Chem. 11 (1973) 2813–2845.
[48] G. Geuskens, M. Kabamba, Photo-oxidation of polymers - part V: a newchain scission mechanism in polyolefins, Polym. Degrad. Stab. 4 (1982) 69–76.
[49] M. Iring, F. Tudos, Thermal oxidation of polyethylene and polypropylene:effects of chemical structure and reaction conditions on the oxidation process, Prog. Polym. Sci. 15 (1990) 217–262.
[50] J. Hernández-Fernandez, E. Rodríguez, Determination of phenolic antioxidants additives in wastewater from polypropylene production using solid-phase extraction with high performance liquid chromatography, J. Chromatogr. A 2019 (1607) 460442–460448.
[51] J. Hernández-Fernández, E. Rayón, J. López, M. Arrieta, Enhancing the thermal stability of polypropylene by blending with low amounts of natural antioxidant, Macromol. Mater. Eng 304 (2019) 1900379–1900391.
[52] J. Hernández-Fernández, J. López, Experimental study of the auto-catalytic effect of triethylaluminum and TiCl4 residuals at the onset of non-additive polypropylene

degradation and their impact on thermo-oxidative degradation and pyrolysis, J. Anal. Appl. Pyrolysis 155 (2021) 105052–105064.
[53] J. Suh, N. Kang, J. Lee, Direct determination of arsine in gases by inductively coupled plasma–dynamic reaction cell–mass spectrometry, Talanta 78 (2009) 321–325.
[54] L. Helsen, Sampling technologies and air pollution control devices for gaseous and particulate arsenic: a review, Environ. Pollut. 137 (2005) 305–315.
[55] M. Pantsar-Kallio, A. Korpela, Analysis of gaseous arsenic species and stability studies of arsine and trimethylarsine by gas chromatography-mass spectrometry, Anal. Chim. Acta 410 (2000) 65–70.
[56] R. Firor, B. Quimby, Dual-Channel Gas Chromatographic System for the Determination of Low-level Sulfur in Hydrocarbon Gases, Agilent Technologies Application Note 5988-8904EN, Agilent Technologies publisher, Wilmington, Delaware, USA, 2003.
[57] M. Pantsar-Kallio, P. Manninen, Simultaneous determination of toxic arsenic and chromium species in water samples by ion chromatography-inductively coupled plasma mass spectrometry, J. Chromatogr. A 779 (1997) 139–146.
[58] G. Lopez, M. Artetxe, M. Amutio, J. Bilbao, M. Olazar, Thermochemical routes for the valorization of waste polyolefinic plastics to produce fuels and chemicals a review, Renew. Sustain. Energy Rev. 73 (2017) 346–368.
[59] C. Pavon, M. Aldas, J. López-Martínez, J. Hernández-Fernández, M. Arrieta, Films based on thermoplastic starch blended with pine resin derivatives for food packaging, Foods 10 (2021) 1171–1186.
[60] C. Pavon, M. Aldas, J. Hernandez-Fernandez, J. Lopez-Martínez, Comparative characterization of gum rosins for their use as sustainable additives in polymeric matrices, J. Appl. Polym. Sci. (2021) 51734–51743.
[61] J. Hernández-Fernández, J. López, D. Barcelo, Development and validation of a methodology for quantifying parts-per-billion levels of arsine and phosphine in nitrogen, hydrogen and liquefied petroleum gas using a variable pressure sampler coupled to gas chromatography-mass spectrometry, J. Chromatogr. A 2021 (1637) 461833–461844.
[62] J. Hernández-Fernández, Quantification of arsine and phosphine in industrial atmospheric emissions in Spain and Colombia. Implementation of modified zeolites to reduce the environmental impact of emissions, Atmospheric Pollut. Res. 12 (2021) 167–176.
[63] J. Hernández-Fernández, J. López, D. Barcelo, Quantification and elimination of substituted synthetic phenols and volatile organic compounds in the wastewater treatment plant during the production of industrial scale polypropylene, J. Chromatogr. A 263 (2021) 128027–128038.